MODELING OF THE THERMAL STABILITY OF AVIATION FUELS

G.V. Deshpande, Michael A. Serio, Peter R. Solomon, and Ripudaman Malhotra*

Advanced Fuel Research, Inc.
87 Church Street
East Hartford, CT 06108

*SRI International
333 Ravenswood Avenue
Menlo Park, CA 94025

INTRODUCTION

The detailed chemical reactions that result in fuel deposits are very complex and very poorly understood at the present. However, it has been reported by several researchers (1-6) that the reaction usually initiates with a liquid phase oxidation of the fuel, which is promoted by dissolved oxygen. Common impurities such as compounds of sulfur, nitrogen, and dissolved metals play a role by either accelerating the reactions or affecting the solubility of the degradation products. Above 750 K, the deposition reaction is characterized by the pyrolysis of hydrocarbon molecules and the scission of hydrogen.

Mayo and Lan (2) have studied the rates of oxidation and gum formation for different fuels. They used t-BU_2O_2 as the initiator and found that some fuels oxidized faster at 100°C than in their previous work (7) at 130°C without initiator. They proposed that gum formation starts with coupling of two alkyl peroxy radicals in the chain termination of oxidation and that growth beyond dimer depends on converting dimer to peroxy radicals by chain propagation.

The general free radical mechanism agreed upon by several researchers and outlined by Foder et. al. (5) is given below.

Formation of alkyl peroxide:	$RH + O_2 \text{ ----> } ROOH$	(1-a)
Initiation:	$ROOH \text{ ----> } HO^{\cdot} + RO^{\cdot}$	(1-b)
Propagation:	$HO^{\cdot} + RH \text{ ----> } R^{\cdot} + H_2O$	(1-c)
	$RO^{\cdot} + RH \text{ ----> } R^{\cdot} + ROH$	(1-d)
	$R^{\cdot} + O_2 \text{ ----> } RO_2^{\cdot}$	(1-e)
	$RO_2^{\cdot} + RH \text{ ----> } R^{\cdot} + ROOH$	(1-f)
Termination:	$RO_2^{\cdot} + RO_2^{\cdot} \text{ ----> Products}$	(1-g)
	$R^{\cdot} + R^{\cdot} \text{ ----> } R - R$	(1-h)

A study was done at Advanced Fuel Research, Inc. (AFR) in which Fourier Transform Infrared Spectroscopy (FT-IR) and Field Ionization Mass Spectrometry (FIMS) were used to study the products from fuel degradation (soluble gums, insoluble gums, and deposits removed on a wire collection probe) (8). The results indicated that the wire deposits were primarily long chain aliphatics (heavier than the starting fuel), which may be formed by termination steps in the above mechanism. The soluble gums were primarily lower molecular weight aliphatics and aromatics which are likely formed by the main decomposition steps. The insoluble gums were intermediate in character, although more closely resembled the wire deposits.

A detailed thermal stability model will require study of additional fuels over a wide range of conditions. A preliminary global model was developed to describe the processes influencing deposition by extending work done at the United Technologies Research Center (UTRC) (4). The UTRC model employed two steps to describe decomposition, step 1 in which fuel plus oxygen is converted into a precursor for deposit formation and step 2 in which the precursor is converted to deposit. We have added a third step for the decomposition of the precursor back to fuel and CO_2. In addition, we have added a mass transport step which can limit the transport of the precursor to the wall surfaces.

MODEL DEVELOPMENT

Because of the difficulty in applying the detailed deposition mechanism cited in Eqs. (1-a) through (1-h) to a multi-component fuel, global reaction mechanisms are often postulated. A global model is also more appropriate for input into a comprehensive code which also includes fluid mechanics and heat transfer.

A two-step kinetic reaction mechanism has been postulated by Giovanetti and Szetela (4) and has been successfully applied to a number of time-temperature histories of the jet fuels. There are two major drawbacks of the model: 1) It does not consider any mass transfer effects; 2) It does not have possible precursor decomposition reactions which will be relevant at high temperatures.

Marteney and Spadaccini (9) have reported deposition rates for a wide temperature range and have found that at temperatures above 645 K, there is a sudden decrease in the deposition rate. A similar trend has been found by Taylor (10). This sudden drop could be due to possible mass transfer resistances at high temperatures and/or precursor decomposition. Marteney and Spadaccini (9) also studied the effect of fuel flow rate on the deposition rate. They found that the peak deposition rate occurred at a lower temperature in laminar flow, suggesting that the reaction became mixing limited at elevated temperatures.

Clark and Thomas (11) found evidence that a fuel's behavior in the JFTOT may be dominated by physical transport or chemical reaction processes and that the relative importance of these two factors is fuel dependent. They found that the weight of the carbon deposited per unit flow rate went through a maximum as the flow rate was increased from 1 ml/min to 11 ml/min. They have explained their results by 3 possible rate limiting steps and postulated that the time constant of each step is fuel and flow rate dependent.

The following summary can be made of the observations on field deposition from the experimental data reported in literature.

1. The deposition rate goes through a maximum with temperature.

2. The deposition rate goes through a maximum with length of the tube.

3. The deposition rate at low temperatures declines with prestressing.

4. The deposition rate at high temperatures does not change with prestressing.

5. The pressure does not appear to exert any influence on the deposition rate.

6. The deposition rate changes with flow rate and time of the experiment. Based on these observations the following global fuel oxidation and deposition model is proposed.

$$\text{Fuel} + O_2 \xrightarrow{K_1} \text{Precursor} + \text{Fuel} \qquad (2\text{-a})$$

$$\text{Precursor} + \text{Fuel} \xrightarrow{K_2} \text{Deposit} + \text{Fuel} \qquad (2\text{-b})$$

$$\text{Precursor} + \text{Fuel} \xrightarrow{K_3} \text{Fuel} + CO_2 \qquad (2\text{-c})$$

It is assumed that reactions 2-a and 2-b occur in the bulk and reaction 2-c occurs on the inner wall surface. For laminar flow, a stagnant layer exists in the vicinity of the wall and the mass transfer resistance may be significant for the precursor.

The time rates of change of the active species are given by

$$d[O_2]/dt = - K_1 [\text{fuel}] [O_2] \qquad (3\text{-a})$$

$$d[\text{precursor}]/dt = K_1 [\text{fuel}] [O_2] - K_3 [\text{precursor}] [\text{fuel}] - R_m \qquad (3\text{-b})$$

$$d[\text{deposit}]/dt = K_2 [\text{fuel}] [\text{precursor}]_s \qquad (3\text{-c})$$

where the brackets [] denote concentration in moles/cc and the subscript s denotes the concentration at the inner surface of the tube. The mass transfer rate, R_m is given by

$$R_m = K_m \bullet S \bullet ([\text{precursor}] - [\text{precursor}]_s) \qquad (4\text{-a})$$

where K_m is the mass transfer coefficient (cm/sec) and s is surface area per unit volume (cm^{-1})

$$S = 4/d \qquad (4\text{-b})$$

where d is the inner diameter of the tube.

If we equate the mass transfer rate to the deposition rate (assuming steady state), we get

$$R_m = K_{EFF} \bullet [\text{precursor}] \qquad (4\text{-c})$$

where K_{EFF} is given by the following equation

$$1/K_{EFF} = 1/K_2/[\text{fuel}] + d/4/K_m \qquad (4\text{-d})$$

The mass transfer coefficient, K_m is estimated by using heat transfer analogy.

The Nusselt number for heat transfer for laminar flow is given by the Seider-Tate equation (12). The Nusselt number for mass transfer can be written as

$$Nu_{AB} = 1.86\ Re^{1/3}\ Sc^{1/3}\ (d/L)^{1/3} \qquad (5\text{-a})$$

where Re and Sc are the Reynolds and Schmidt numbers, respectively, and L is the length of the tube.

Marteney and Spadaccini (9) have given the heat transfer characteristics of JP-5 and found that for the transition and turbulent region, a simple Dittus-Boelter equation could be used to describe the heat transfer characteristics.

Thus for the non-laminar region, the Nusselt number for mass transfer can be written as

$$Nu_{AB} = 0.023\ Re^{0.8}\ Pr^{0.4} \qquad (5\text{-b})$$

The mass transfer coefficient, K_m is then given by the following equation

$$K_m = Nu_{AB} \bullet D^{\circ}_{AB}/d \qquad (5\text{-c})$$

where D°_{AB} is the binary diffusivity of the precursor-fuel system.

The binary diffusivity can be estimated by Wilke and Chang (13,14) as follows

$$D^{\circ}_{AB} = \frac{(117 \cdot 3 \times 10^{-18})\ (Q\ M_B)^{0.5} T}{\mu \nu_A^{0.6}} \qquad (6)$$

where D°_{AB} = diffusivity of A in very dilute solution in Solvent B, m^2/s, M_B = molecular weight of solvent, kg/kmol, T = temperature, K, μ = solution viscosity, $kg/m \cdot ^5$, ν_A = solute molar volume at normal boiling point, m^3/kmol, Q = association factor for solvent and is 1.0 for unassociated solvents. ν_A can be estimated from the molecular formula of the diffusing species and the values of atomic and molecular volumes (15).

MODEL PREDICTIONS

The experimental data used in the modeling has been taken from the NASA report by Giovanetti and Szetela (4). As discussed above, they had proposed a two-step reaction model. Their model curves are compared with the experimental data for three cases in Figs. 1a, 2a, 3a, respectively. The experimental data of Fig. 2a was used to calibrate the model and hence the fit to it is the best of the three cases. There was a discrepancy in the UTRC model. In order to fit the data, the initial oxygen concentration in fuel was assumed to be 16% of the saturation value. In addition, the mass transfer effects and precursor decompositions, which yield lower deposit formation rates at high temperatures were also neglected.

The results of the simulation of the model which included mass transfer effects are shown in Figs. 1b, 2b, and 3b. It can be seen that the model underpredicts the deposit formation at high temperatures where mass transfer effects are likely to be important. At low temperature, the model predictions are slightly improved. Thus even at the low temperature, some mass transfer resistance is present due to the very low velocity used in this experiment.

When the model constants were fitted in the UTRC work, the mass transfer effects were neglected and hence the frequency factor and activation energy for the deposit formation reaction were the global rate instead of the true kinetic rate. Consequently, in order to fit the data with mass transfer, the frequency factor or activation energy had to be changed. In addition, the initial oxygen concentration was made equal to the saturation value. The frequency factor of the reaction for deposit formation was kept constant and the activation energy was increased from 31,000 kcal/mole to 32,600 kcal/mole. The results of these simulations are given in Figs. 1c, 2c, and 3c, respectively. By this change, the experimental data at low temperature (low velocity) and high temperature (high velocity) were predicted

very well but the data at high temperature (low velocity) showed a leveling effect after distance of 60 cm and the model predicted an increasing trend of deposit formation even at distance of 120 cm.

The above observation suggested that the leveling off of the deposit formation is due to the precursor decomposition. This would also explain the trend of lower deposit formation at higher temperatures. A third reaction of precursor decomposition was incorporated in the model with the activation energy of 32,600 and frequency factor of 2.0×10^{14}. The results of these simulations are given in Fig. 1d, 2d, and 3d, respectively. **The model now seems to predict the data very well for all the three cases.**

Giovanetti and Szetela (4) have also measured the deposit formation for the fuel Suntech A. The major differences between fuel Jet A and the fuel Suntech A are in the organic oxygen content, the aromatic and paraffins content and in the amount of trace elements. Based on the speculations of the various researchers reported in literature, Suntech A would be more reactive fuel that Jet A and consequently deposit formation will be higher than Jet A under identical stressing conditions. This kind of behavior was found by Giovanetti and Szetela (4) and it was reported that the carbon deposition rates for Suntech A were as high as a factor of ten greater than those for Jet A.

The UTRC model and the AFR model were exercised over two time-temperature histories for Suntech A. The deposit formation was underpredicted, which is attributed to the higher reactivity of Suntech A than Jet A. The fuel reactivity would influence the rate of the precursor formation and possibly of deposit formation. Hence the rates of these reactions were increased 40 times by increasing the frequency factor. The results of these simulations are shown in Figs. 4a and 4b. The low temperature deposit formation is predicted very well but the high temperature data are underpredicted.

Since Suntech A had a higher organic oxygen content than Jet A and the chemical composition was different (i.e. more aromatic than Jet A), the oxygen solubility and/or initial precursor concentration could be different. In our model, the initial precursor concentration is assumed to be zero. Hence the initial oxygen concentration was doubled and the rates of precursor and deposit formation were increased 20 times in the Jet A parameters. The results of these simulations are shown in Figs. 4c and 4d. The low temperature data is predicted equally well but the predictions at high temperatures are greatly improved. This result suggests that the knowledge of precursor concentration in the fuel may be important and the deposit formation may be greatly enhanced if the oxygen solubility in the fuel is higher and/or the fuel contains oxygenated species to begin with.

Sensitivity Analysis - The AFR model is a three reaction model which also includes mass transfer effects. A preliminary sensitivity analysis for the reaction parameters was done by varying the frequency factor so that the rate constants were increased by an order of magnitude on either side of the base case. The mass transfer effects were studied by varying the diffusivity.

(a) Variations in Diffusivity - This was achieved by varying the constant in the Stokes-Einstein (16) equation ($D_{AB}\mu_B/T$ = Constant). The base case used for the sensitivity analysis was that of fuel Jet A under high temperature and low velocity conditions where the mass transfer effects will have the maximum impact on deposit formation. Since the binary diffusivity of the precursor in the fuel is estimated by correlation, the sensitivity of this estimation was done and is shown in Fig. 5a. **The effect of increasing the diffusivity significantly increases the amount of deposit formation and this clearly shows the base case chosen is mass transfer limited as expected.**

(b) Variations in A(1) - The rate constant, K_1, of the reaction forming precursor was varied by varying the frequency factor. The results are shown in Fig. 5b. It is interesting to note that lowering the rate constant by an order of magnitude results in significantly lowering the amount of deposit formation but increasing by an order of magnitude does not change the amount of deposit formation very much. **This suggests that the precursor formation rate is not always limiting the deposition process.**

(c) Variations in A(2) - The rate constant, K_2, of the reaction forming deposit was varied by varying the frequency factor. The results are shown in Fig. 5c. An effect similar to that observed for the variation of K_1 is seen for variation of K_2. Even though K_2 was increased by an order of magnitude, the amount of deposit formation did not increase very much. This reinforces the fact that the base case is mass transfer limited. Lowering of K_2, however, did decrease the amount of deposit formation.

(d) Variations in A(3) - The rate constant, K_3, of the reaction involving precursor decomposition was varied by varying the frequency factor. The results are shown in Fig. 5d. Since increasing this rate reduces the precursor concentration, the deposit formation is reduced. Lowering the rate by an order of magnitude does not increase the deposit formation by a large amount but increasing the rate did decrease the deposit formation.

Predictions of AFR Data - The results shown in Fig. 6 show that the model can predict the maximum in deposit measured in our experiments (8,17). This maximum cannot be predicted by the UTRC model.

SUMMARY

A preliminary global model was developed extending the work done at UTRC. This new model which includes mass transfer and a precursor decomposition step can predict variations in deposit formation with fuel type, flow rate, residence time, and temperature-time history. This initial modeling effort has indicated that the measurement of the deposit precursors in addition to the deposit formation is clearly needed for model discrimination purposes. The use of on-line FT-IR diagnostics used in a related study (8,17) will help to identify the different precursors and their concentration behavior with temperature and residence time.

ACKNOWLEDGEMENTS

The authors wish to acknowledge the support of the U.S. Air Force (Aero Propulsion Laboratory, Wright Aeronautical Laboratories, Aeronautical Systems Division, Wright-Patterson AFB, Ohio) under Contract No. F33615-88-C-2853. We are also grateful to Dr. Pierre Marteney of the United Technologies Research Center (UTRC), East Hartford, CT who supplied copies of past UTRC reports on modeling of thermal stability.

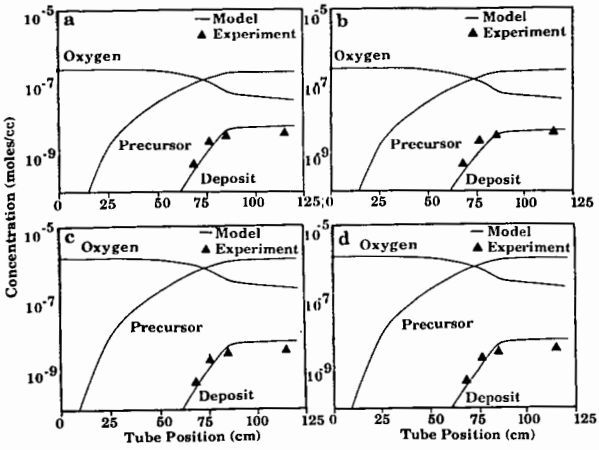

Figure 1. Predicted and Measured Deposit Species Concentration - Tube Position Histories for Jet A Flowing in a Heated Tube - Low Temperature and Low Velocity Condition. a) UTRC Model (O_2) init = 2.25E-7 moles/cc, E(2) = 31,000 cals/gmole, E(3) = 0 cals/gmole, b) AFR Model (O_2) init = 2.25E-7 moles/cc, E(2) = 31,000 cals/gmole, E(3) = 0 cals/gmole, c) AFR Model (O_2) init = 1.40E-6 moles/cc, E(2) = 32,600 cals/gmole, E(3) = 0 cals/gmole, and d) AFR Model (O_2) init = 1.40E-6 moles/cc, E(2) = 32,600 cals/gmole, E(3) = 32,600cals/gmole. Data from Ref. 4.

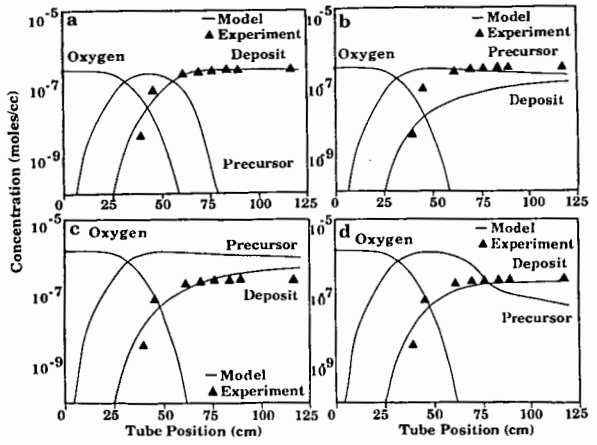

Figure 2. Predicted and Measured Deposit Species Concentration - Tube Position Histories for Jet A Flowing in a Heated Tube - High Temperature and Low Velocity Condition. a) UTRC Model (O_2) init = 2.25E-7 moles/cc, E(2) = 31,000 cals/gmole, E(3) = 0 cals/gmole, b) AFR Model (O_2) init = 2.25E-7 moles/cc, E(2) = 31,000 cals/gmole, E(3) = 0 cals/gmole, c) AFR Model (O_2) init = 1.40E-6 moles/cc, E(2) = 32,600 cals/gmole, E(3) = 0 cals/gmole, and d) AFR Model (O_2) init = 1.40E-6 moles/cc, E(2) = 32,600 cals/gmole, E(3) = 32,600cals/gmole. Data from Ref. 4.

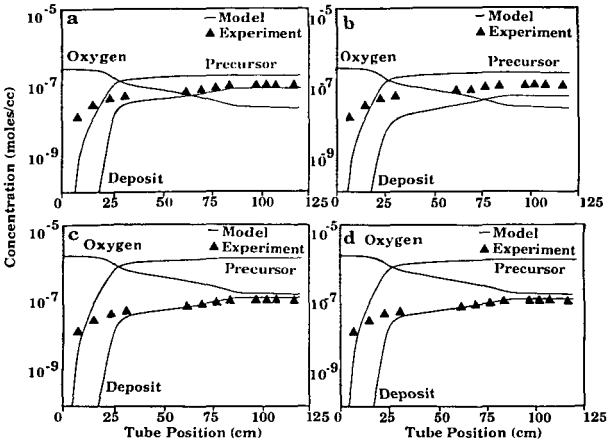

Figure 3. Predicted and Measured Deposit Species Concentration - Tube Position Histories for Jet A Flowing in a Heated Tube - High Temperature and High Velocity Condition. a) UTRC Model (O_2) init = 2.25E-7 moles/cc, E(2) = 31,000 cals/gmole, E(3) = 0 cals/gmole, b) AFR Model (O_2) init = 2.25E-7 moles/cc, E(2) = 31,000 cals/gmole, E(3) = 0 cals/gmole, c) AFR Model (O_2) init = 1.40E-6 moles/cc, E(2) = 32,600 cals/gmole, E(3) = 0 cals/gmole, and d) AFR Model (O_2) init = 1.40E-6 moles/cc, E(2) = 32,600 cals/gmole, E(3) = 32,600cals/gmole. Data from Ref. 4.

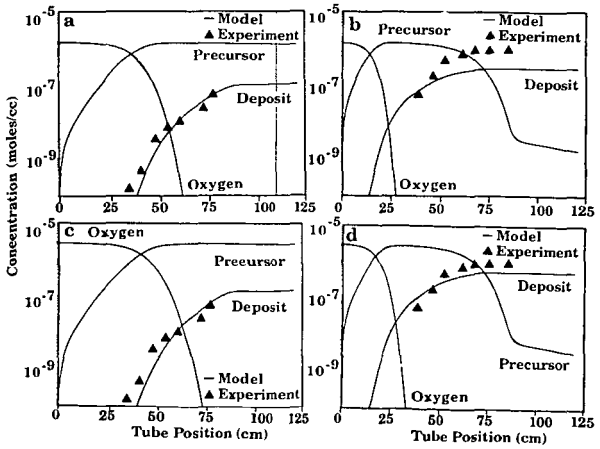

Figure 4. Predicted and Measured Deposit Species Concentration - Tube Position Histories for Suntech A Flowing in a Heated Tube - Low Velocity Condition. E(1) = 17,000 cals/gmole, E(2) = 32,600 cals/gmole, E(3) = 32,600 cals/gmole and A(3) = 0.2 E15. a and c are Low Temperature and b and d are High Temperature Conditions. a and b) (O_2) init = 1.40E-6 moles/cc, A(1) = 0.14E12, A(2) = 0.8E16 and c and d) (O_2) init = 2.80E-6 moles/cc, A(1) = 0.07E12, A(2) = 0.4E16. Data from Ref. 4.

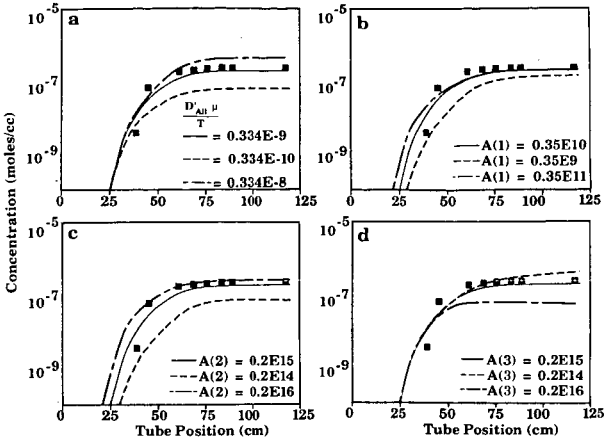

Figure 5. Effect on Deposit Formation of: a) Diffusivity, D_{AB}, b) Rate Constant, k_1, c) Rate Constant, k_2, and d) Rate Constant, k_3 for Fuel Jet A under High Temperature and Low Velocity Conditions. Base Case: $D_{AB}\mu/T$ = 0.334E-9, A(1) = 0.35E10, A(2) = 0.2E15, A(3) = 0.2E15. Data from Ref. 4.

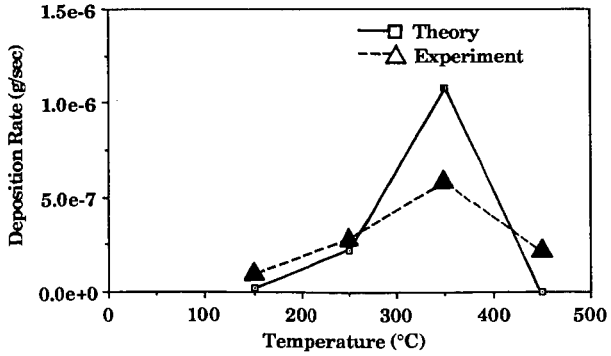

Figure 6. Comparison of AFR Model Predictions with Deposition Rate for Aerated JP-5.

REFERENCES

1. Kendall, D.R. and Mills, J.S., Ind. Eng. Chem. Prod. Res. Dev., **25**, 360 (1986).
2. Hazlett, R.N., "Free Radical Reactions Related to Fuel Research," in Frontiers of Free Radical Chemistry, William A. Pyror (Ed.), Academic Press,New York, pp. 195-223 (1980).
3. Mayo, F.R. and Lan, B.Y., Ind. Eng. Chem. Res., **25**, 333, (1986).
4. Giovanetti, A.J., and Szetela, E.J., "Long Term Deposit Formation in Aviation Turbine Fuel at Elevated Termperature", NASA Final Report, Contract No. NAS3-24091, (1985).
5. Fodor, G.E., Energy and Fuel, **2**, 729, (1988).
6. Reddy, K.T. and Cerransky, N.P., Energy and Fuel, **2**, 205, (1988).
7. Tseregounis, S.I., Spearot, J.A. and Kite, D.J., Ind. Eng. Chem. Res., **26**, 886 (1987).
8. Serio, M.A., Malhotra, R., Kroo, E., Desphande, G.V., Solomon, P.R., "A Study of the Thermal Stability of JP-5 using FT-IR and FIMS" paper to be presented at the Symposium on the structure of Future Jet Fuels II, Division of Petroleum Chemistry, ACS Miami Meeting, Sept. 10-15, 1989.
9. Marteney, P.J. and Spadaccini, L.J., Journal of Eng. For Gas Turbines and Power, **108**, 648, (1986).
10. Taylor, W.F., IEC Product Res. Dev., **8**, 375, (1965).
11. Clark, R.H. and Thomas, L., "An Investigation of the Physical and Chemical Factors Affecting the Performance of Fuels in The JFTOT", presented at the SAE Aerospace Technology Conf. and Exposition, Anaheim, CA, (1988).
12. Sieder, E.N. and Tate, G.E., Ind. Eng. Chem. **28**, 1429, (1936).
13. Wilke, C.R., Chem. Eng. Progr., **45**, 218, (1949).
14. Wilke, C.R., and Chang, P., AIChE, J., **1**, 264, (1965).
15. Treybal, R.E., Mass Transfer Operations, McGraw Hill, p. 333, (1980).
16. Sheldon, R.A. and Kochi, J.K., Metal-Catalyzed Oxidations of Organic Compounds, Academic Press, NY, (1981).
17. Serio, M.A., Malhotra, R., Kroo, E., Deshpande, G.V., Solomon, P.R., "Thermal Stability of Aviation Fuels", Final Report for Contract F33615-88-C-2853, March, 1989.